Neuro-Oncology Advances
2(1), 1–9, 2020 | doi:10.1093/noajnl/vdaa132 | Advance Access date 16 October 2020

RNAi technology targeting the *FGFR3-TACC3* fusion breakpoint: an opportunity for precision medicine

Brittany C. Parker Kerrigan, Daniel Ledbetter, Matthew Kronowitz, Lynette Phillips, Joy Gumin, Anwar Hossain, Jing Yang, Mayela Mendt, Sanjay Singh, David Cogdell, Chibawanye Ene, Elizabeth Shpall, and Frederick F. Lang

Department of Neurosurgery, The University of Texas MD Anderson Cancer Center, Houston, Texas, USA (B.C.P.K., D.L., M.K., L.P., J.G., A.H., J.Y., S.S., C.E., F.F.L.); Brain Tumor Center, The University of Texas MD Anderson Cancer Center, Houston, Texas, USA (B.C.P.K., D.L., M.K., L.P., J.G., A.H., J.Y., S.S., C.E.); Department of Stem Cell Transplantation, The University of Texas MD Anderson Cancer Center, Houston, Texas, USA (M.M., E.S.); Department of Pathology, The University of Texas MD Anderson Cancer Center, Houston, Texas, USA (D.C.)

Corresponding Author: Frederick F. Lang, MD, Department of Neurosurgery, Unit 442, The University of Texas MD Anderson Cancer Center, 1515 Holcombe Blvd., Houston, TX 77030, USA (flang@mdanderson.org).

Abstract

Background. Fusion genes form as a result of abnormal chromosomal rearrangements linking previously separate genes into one transcript. The FGFR3-TACC3 fusion gene (F3-T3) has been shown to drive gliomagenesis in glioblastoma (GBM), a cancer that is notoriously resistant to therapy. However, successful targeting of F3-T3 via small molecular inhibitors has not revealed robust therapeutic responses, and specific targeting of F3-T3 has not been achieved heretofore. Here, we demonstrate that depleting F3-T3 using custom siRNA to the fusion breakpoint junction results in successful inhibition of F3-T3+ GBMs, and that exosomes can successfully deliver these siRNAs.

Methods. We engineered 10 unique siRNAs (iF3T3) that specifically spanned the most common F3-T3 breakpoint with varying degrees of overlap, and assayed depletion by qPCR and immunoblotting. Cell viability assays were performed. Mesenchymal stem cell–derived exosomes (UC-MSC) were electroporated with iF3T3, added to cells, and F3-T3 depletion measured by qPCR.

Results. We verified that depleting F3-T3 using shRNA to FGFR3 resulted in decreased cell viability and improved survival in glioma-bearing mice. We then demonstrated that 7/10 iF3T3 depleted F3-T3, and importantly, did not affect levels of wild-type (WT) FGFR3 or TACC3. iF3T3 decreased cell viability in both F3T3+ GBM and bladder cancer cell lines. UC-MSC exosomes successfully delivered iF3T3 in vitro, resulting in F3-T3 depletion.

Conclusion. Targeting F3-T3 using siRNAs specific to the fusion breakpoint is capable of eradicating F3T3+ cancers without toxicity related to inhibition of WT FGFR3 or TACC3, and UC-MSC exosomes may be a plausible vehicle to deliver iF3T3.

Key Points

- RNAi to the F3-T3 breakpoint (iF3T3) robustly depletes F3-T3, resulting in tumor cell death.
- iF3T3 spares WT FGFR3 and TACC3, mitigating normal tissue toxicities.
- MSC-derived exosomes successfully deliver iF3T3, resulting in functional F3-T3 depletion.

Importance of the Study

This study provides initial evidence for the feasibility and efficacy of using siRNA to specifically target the F3-T3 fusion breakpoint as a treatment of tumors harboring F3-T3 fusions. We demonstrate that this strategy robustly depletes F3-T3 RNA and protein, resulting in decreased cell viability. We illustrate this effect in both F3-T3+ GBM and bladder cancer cell lines. Importantly, we illustrate that WT FGFR3 and TACC3 are spared by this treatment, which provides immense benefit in the context of normal tissue toxicities commonly associated with small molecular inhibitors. Therefore, iF3T3 holds potential as a "silver bullet" strategy for the treatment of F3-T3+ cancers because it specifically targets the fusion breakpoint, resulting in cell death while avoiding normal tissue toxicity.

Fusion genes form as a result of chromosomal translocations, inversions, or deletions of intervening sequences that reposition portions of 2 different genes into a single transcript. Chimeric fusion proteins have been identified as potent oncogenes in various cancers.[1,2] The first identified fusion was the *breakpoint cluster region protein-abelson murine leukemia viral oncogene homolog 1* fusion gene, or "*BCR-ABL*," which is found in chronic myeloid leukemia.[3,4] Therapeutic targeting of this fusion has been successfully achieved by targeting ABL kinase using the kinase inhibitor imatinib, which leads to remission in a majority of CML cases, although resistance is common, and normal tissue toxicities occur.[4] Fusions have also been identified in several solid tumors. For example, the *EML4-ALK* fusion is found in up to 4% of non-small cell lung cancers,[5] and has been targeted with ALK tyrosine kinase inhibitors.[6–8]

The *FGFR3-TACC3* (F3-T3) fusion has emerged as an oncogenic driver in a variety of cancers, most notably glioblastoma (GBM), in which F3-T3 fusions were first identified,[9–11] as well as bladder, cervical, lung, and nasopharyngeal cancers.[9–16] The detection and characterization of the F3-T3 fusion in up to 4% of GBMs has presented a rare opportunity for personalized medicine in this recalcitrant cancer, which has a median survival of only 14 months despite maximal surgery, radiation, and chemotherapy.[17] Indeed, there are currently no personalized therapeutics for GBM; therefore, developing an F3-T3-specific agent would be a major advance in personalized medicine in GBM. Such a therapeutic would also be applicable to the other cancers harboring F3-T3 fusions.

The F3-T3 fusion forms via tandem duplication of a 70-kb region on chromosome 4p16.3 and is found exclusively in tumor cells. Forced expression of F3-T3 in preclinical models accelerated tumor growth, indicating the F3-T3 fusion is a powerful oncogene,[9,10] and a logical anti-GBM therapeutic target. However, targeting the fusion is complicated by the fact that wild-type (WT) TACC3 is present in normal brain. Although WT FGFR3 levels are low in normal brain, it is found in multiple peripheral organs; therefore, targeting FGFR3 can lead to normal tissue toxicity.

In this context, a variety of small molecules have been developed to inhibit the FGFR kinase domain and have been utilized to target F3-T3-positive cancers. Results from an open-label, multicenter, phase II study with the primary endpoint being 6-month progression-free survival (PFS) were recently published on a selective small-molecule pan-FGFR kinase inhibitor, Infigratinib. In this study, 26 patients were treated with 21 patients (96%) discontinuing treatment due to disease progression and 3 patients for other reasons. The median PFS was 1.7 months, and median overall survival was 6.7 months, with the best overall response being a partial response in 7.7% of patients.[18] Treatment-related adverse events (AEs), including hypophosphatemia, fatigue, and diarrhea resulted in dose interruptions or reductions in about 42% of patients. Similarly, broadly targeted, multi-tyrosine kinase inhibitors, such as dovitinib, have been evaluated for treatment F3-T3-positive and WT FGFR3 gliomas. Sharma et al. reported minimal effect of dovitinib across various patient cohorts (0%–6% PFS-6 and a median time of 1.8 months to progression), regardless of FGFR3 mutation status. Similar to infigratinib, dovitinib was associated with serious AEs, including thrombocytopenia (70%) and thromboembolic events (42%).[19]

It is important to consider that the 6-month PFS for recurrent GBM treated with lomustine, a nitrosurea-based chemotherapy most commonly used for recurrent GBM, is 19%.[20] Although a phase III clinical trial is needed to compare the efficacy of infigratinib and dovitinib to agents such as lomustine, results from these phase II clinical trials indicate that pan-FGFR inhibitors do not provide significant clinical benefit relative to current treatments, but importantly have clinically consequential side effects related to off-target and/or on-target off-tissue interactions of the drugs. Therefore, there remains an urgent need to develop a targeted agent that selectively inhibits tumor cells harboring the oncogenic F3-T3 fusion while sparing healthy tissue that express WT FGFR3 or TACC3. In this context, the fusion breakpoint is a unique sequence found only in tumor cells and not in normal cells. Therefore, we sought to develop potent and precise therapies to specifically target the F3-T3 fusion breakpoint, thereby circumventing side effects associated with targeting WT FGFR3 or TACC3. To this end, we designed RNAi specific to the F3-T3 breakpoint sequence, which we refer to as iF3T3. We reasoned that iF3T3 specifically encompasses the fusion breakpoint and therefore would not target WT FGFR3 or TACC3, and because F3-T3 is not found within normal tissues.

Because naked RNA is degraded in blood and lacks directionality to organs of interest, we explored various delivery mechanisms that both direct iF3T3 to its target destination and protect it along the way. Specifically, we employed exosomes, which are nanovesicles released from

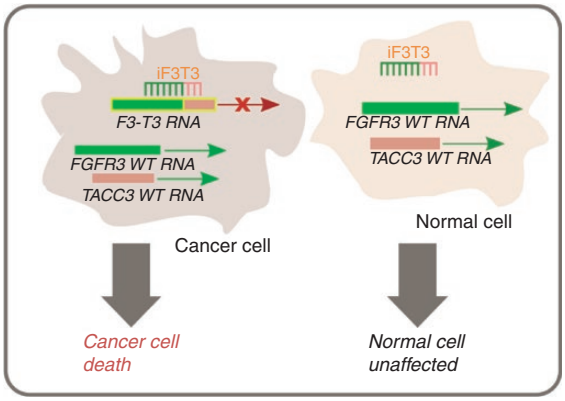

Figure 1. Overview of study rationale and goals. The iF3T3 strategy involves specific targeting of the fusion breakpoint sequence that does not recognize WT FGFR3 or TACC3 RNA. The F3T3 fusion is not present in normal cells, and therefore normal cells are unaffected.

cells under normal physiological conditions that are stable in blood due to their lipid bilayer coat. We chose to use exosomes derived from mesenchymal stem cells (MSCs), as we have previously shown that these cells and their exosomes exhibit the unique property of homing to brain tumors following systemic administration.[21–25]

Therefore, the overall goal of this work was to explore the extent to which iF3T3, an siRNA specific to the breakpoint sequence, would result in degradation of F3-T3 RNA leading to cell death without undo side effects due to nonspecifically targeting WT FGFR3 and TACC3 (Figure 1). We also undertook initial studies to determine whether this therapeutic could be delivered to tumor cells via MSC-derived exosomes. Because the F3-T3 fusion occurs in a vast variety of cancer types, development of this therapeutic holds the potential to significantly impact patient outcomes across the cancer spectrum.

Methods

Constructs

FGFR3-TACC3 fusion and WT FGFR3 constructs were generated in the pcDNA3.1 plasmid backbone as previously described.[9] Plasmids for expression of shRNA targeting WT FGFR3 were purchased (Dharmacon Cat. RHS4533-EG2261). Custom shRNA and siRNA targeting the F3-T3 fusion breakpoint (FGFR3 exon 18 – TACC3 exon 11 (iF3T3; see Figure 2a for sequence) were generated (Dharmacon).

Cell Line Generation and Maintenance

Adherent glioma cell lines U87 Empty Vector "EV," U87.F3T3, U87.WT FGFR3, SNB19.EV, SNB19.F3T3, SNB19.WT FGFR3, and adherent bladder cancer cell line RT112 were cultured in minimum essential medium (MEM) with 10% fetal bovine serum (FBS) and 2 mM L-Glutamine. All glioma stem-like cells (GSCs) were cultured under neurosphere conditions in DMEM/F12 supplemented with B27, EGF (20 ng/mL), FGF (20 ng/mL), and Pen/Strep (100 µg/mL). All cells were maintained at 37°C with 5% CO_2. SNB19.EV, SNB19.F3T3, and SNB19.WT FGFR3 were generated as previously described.[9] The bladder cancer cell line RT112 was generously provided by Dr. Bogdan Czerniak (The University of Texas MD Anderson Cancer Center). U87.F3T3 and U87.EV cell lines were generated as described here.[9] Briefly, 6×10^5 U87-MG cells were transfected with 2.5 µg FGFR3-TACC3 or WT FGFR3 cDNA constructs as previously described[9] or EV pcDNA3.1+ using Lipofectamine 2000 reagent (ThermoFisher) according to the manufacturer's instructions. Stably transfected cells were selected for with complete medium containing 500 µg/mL G418 (Corning) for 14 days. FGFR3 expression was confirmed after expansion of G418-resistant clones by protein isolation followed by western blot.

Detection of Gene Fusion Events in RNA-seq Data

Paired-end sequencing assays were performed on total RNA from GSCs using the Illumina HiSeq platform. Each GSC line generated approximately 50 million 75-bp paired-ends reads. Gene fusion events were determined after mapping FASTQ files to GRCh38_gencode_v31_CTAT_lib_Aug152019 with STAR-Fusion (STAR-Fusion/v1.7.0). All gene pairs with at least one JunctionReadCount for each GSCs are reported in Supplementary Table 1.

Lentivirus Production

Lentiviruses for transduction and expression of shRNA plasmids were generated as follows: HEK293FT cells were transfected with psPAX2, pMD2.G, and shRNA or sh-Control plasmids using Lipofectamine 2000 (ThermoFisher) following manufacturer protocol in Opti-MEM (ThermoFisher). Transfected cells were incubated overnight. Opti-MEM was replaced with DMEM/F12 medium with 10% FBS, 2 mM L-Glutamine, and pen/strep. After 24 h, conditioned media were collected, and media were replaced again. After 24 h, conditioned media were collected and combined with previously collected conditioned media. Virus-containing media were filtered through 0.45 µm filter (EMD Millipore) and ultracentrifuged at 100,000 × *g* for 1 h. Supernatant was removed, pellet was resuspended in phosphate-buffered saline (PBS), and cryopreserved at –80°C.

Cell Viability Assays Following F3-T3 Depletion

U87.F3T3, SNB19.F3T3, and RT112 cells were plated at 1.5×10^5 per well and infected with lentivirus containing sh-F3T3 or sh-Control constructs in Opti-MEM. After 24 h, medium was replaced and after 72 h, cells were trypsinized and replated at 1×10^3 cells per well in 96-well plates. The colorimetric cell proliferation (water soluble tetrazolium salts-1 [WST-1] assay) was performed at each time point following manufacturer instructions. Following incubation of WST reagent, absorbance was measured using BMG

Clariostar microplate reader and data calculations were performed using MARS data analysis software. GSCs were plated at 1 × 10^5 per well and infected with lentivirus containing sh-F3T3 or sh-Control constructs in Opti-MEM. After 24 h, cells were pelleted and medium was replaced. After 72 h, spheres were dissociated with Accutase (Sigma) and replated at 1 × 10^3 cells per well in 96-well plates. CellTiter-Glo (CTG) luminescent cell viability assay (Promega) was performed at each time point according to manufacturer instructions. Following incubation of CTG reagents, luminescence was measured using BMG Clariostar microplate reader, and data calculations were performed using MARS data analysis software.

Reverse Transcription-Quantitative PCR

Glioma cell lines (U87-FGFR3 WT, SNB19.FGFR3 WT, and SNB19.F3T3) were transfected in triplicate with 25 pmol, 100 pmol, or 250 pm siRNA using Lipofectamine 2000 (ThermoFisher #11668027). Forty-eight hours following transfection, cells were lysed in either RIPA buffer with HALT protease and phosphatase inhibitors (ThermoFisher #78447) for protein lysates, or in QIAzol (Qiagen, #79306) for RNA. Total RNA was isolated using the miRNeasy Mini kit (Qiagen # 217004) and quantified using Nanodrop 2000c (check). cDNA was generated with the Superscript III First-Strand Synthesis Kit (ThermoFisher # 18080051) and oligo dT primers. Ten nanograms of cDNA was used per reaction for quantitative PCR with TaqMan Assays GAPDH (hs0275899_g1), FGFR3 (hs00997393_g1), and FGFR3-TACC3 (hs04396817_ft) and TaqMan Universal Master Mix II, no UNG (Applied Biosystems #4440040). Real-time PCR was performed in triplicate using the ABI7500_FAST PCR machine (Applied Biosystems) with the following PCR conditions: 95°C for 10 min followed by 40 cycles of 95°C for 15 s and 60°C for 1 min. GAPDH was used as the internal reference gene, and relative quantitation was calculated using the $2^{-\Delta\Delta Ct}$ method.

Western Blotting

Protein lysates were quantitated by Bradford Assay. Twenty micrograms of total protein was resolved with a 4%–15% gradient gel and protein levels measured by immunoblot using the following antibodies: FGFR3 (sc-13121; Santa Cruz Biotechnology, 1:250), TACC3 (sc-22773 Santa Cruz Biotechnology, 1:1000), and α-tubulin (1:10,000).

In Vivo Experiments

Athymic nude mice (nu/nu) were implanted with glioma cells via cranial guide screw as previously described.[26] All animal manipulations were performed in accordance with ethics guidelines under an approved protocol. Briefly, mice were anesthetized with 0.2 mL ketamine/xylazine cocktail (10 mg/mL ketamine and 1 mg/mL xylazine), and glioma cell suspensions (5 × 10^5 cells in 5 µL sterile PBS) were implanted through cranial guide screws using 26-gauge Hamilton syringes at a rate of 0.5 µL/min by microinfusion syringe pump (Harvard Apparatus). Upon demonstration of behavioral and physical indications of severe morbidity, mice were sacrificed and perfused by intracardiac injection of PBS, followed by 4% paraformaldehyde. Brains were removed and fixed in 10% neutral-buffered formalin prior to paraffin-embedding and sectioning.

Electroporation of Exosomes

Human cord-blood mesenchymal stem cell (MSC)-derived exosomes (Elizabeth Shpall, M.D. Laboratory, Stem Cell Transplantation, M.D. Anderson Cancer Center) were transfected with F3-T3 fusion-specific siRNA (Dharmacon) or control siRNA (Texas Red-labeled Control siRNA, System Bioscience) by electroporation using the Lonza 4D-Nucleofector System. Three micrograms of exosomes were resuspended in Plasmalyte or Lonza Nucleofector buffers and combined with 3 µg F3-T3 siRNA or control siRNA in sterile PBS in Eppendorf tubes. Exosome/siRNA suspensions were mixed gently and transferred to 100 µL Nucleofector cuvettes. Immediately after electroporation, the total reaction volume was transferred to an Eppendorf tube, diluted to 1 mL in serum-free MEM medium, and kept on ice for 10 min. Exosomes were applied dropwise to U87.F3T3 glioma cells in serum-free MEM medium (6 × 10^4 cells per well in 24-well plate) and were swirled gently. After 24 h, medium in each well was replaced with complete U87-MG medium containing 10% FBS and 2 mM L-glutamine. After 72 h incubation, total RNA was isolated from cells for RT-qPCR analysis.

Results

Depleting FGFR3-TACC3 Via shRNA to FGFR3 Results in Decreased Cell Viability and Improved Survival

In order to determine which GSC lines were positive for the fusion, we screened a series of 40 GSCs by qPCR for the fusion and identified 2 F3-T3-positive GSC lines (MDA-GSC13 and MDA-GSC231). These positive cell lines and several negative lines (MDA-GSC326, MDA-GSC400, MDA-GSC17, MDA-GSC309, and MDA-GSC328) were confirmed by either qPCR, western blotting, or RNAseq (Supplementary Figure 1A and B, Supplementary Table 1). We also generated U87-MG cells stably expressing F3-T3 fusion (Supplementary Figures 1 and 4).

We first sought to determine whether fusion depletion via shRNA would serve as a promising therapeutic option. Three sh-FGFR3 lentiviral constructs were utilized: 2 that targeted regions of WT-FGFR3 retained in the fusion and 1 that targeted the 3′ untranslated region (UTR) of WT-FGFR3, which is lost upon formation of the fusion[9] (Supplementary Figure 1C). As expected, lentiviral-mediated infection of fusion-containing cell lines resulted in depletion of F3-T3 and decreased cell viability only when targeting the portion of FGFR3 retained within the fusion (Supplementary Figures 1D and E and 2A and B). Further, ex vivo infection followed by implantation into the brains of athymic mice leads to improved survival upon treatment with fusion-depleting shRNA, while no difference was observed in

negative shRNA controls, or in the F3-T3-negative cell line, MDA-GSC17 (Supplementary Figure 1G and H).

These results together indicate F3-T3 depletion may serve as a viable therapeutic option for F3-T3-positive patients. However, sh-FGFR3-mediated strategies to deplete F3-T3 may yield unwanted toxicities, as this approach also depletes WT FGFR3 (Supplementary Figure 3). Because WT FGFR3 exists in several normal tissues throughout the body, this approach does not avoid normal tissue toxicity[27].

Generation of RNAi to Selectively Deplete F3-T3

Given that the fusion breakpoint results in a uniquely tumor-specific DNA sequence, we sought to determine whether siRNA specific to the fusion breakpoint could selectively deplete F3-T3, while sparing WT FGFR3 or TACC3. To that end, the coding region of the most common F3-T3 breakpoint (FGFR3 exon 18 to TACC3 exon 11) was overexpressed in 2 commercially available GBM cell lines, U87-MG (as previously shown in Supplementary Figure 1) and SNB19 (Supplementary Figure 4A and B). Consistent with previously published literature, overexpression of these F3-T3 constructs in GBM lines results in decreased survival when implanted into the brains of immunocompromised mice (Supplementary Figure 4D and E).[9]

We next designed siRNA spanning the F3-T3 breakpoint, with various degree of overlap (Figure 2A), as we were unsure whether an optimal region existed that would allow successful depletion of F3-T3 RNA while sparing WT FGFR3 and TACC3. The siRNA constructs were transfected into both U87-MG and SNB19 F3-T3-overexpressing cell lines, U87.F3T3 and SNB19.F3T3, respectively, and cells were harvested 48 h later. Immunoblotting confirmed depletion of F3-T3 protein following transfection with each siRNA with individual constructs resulting in varying degrees of degradation (Figure 2B and 2C). Semiquantitative analyses suggested that constructs #5 and #6 seemed to offer the most effective depletion in both cell lines. Because construct #5 had relatively equal overlap of the fusion breakpoint, we reasoned that this construct had the least likely chance of resulting in depletion of WT FGFR3 or TACC3. Therefore, construct #5 was selected for further analysis, and hereafter will be referred to as iF3T3.

RNAi to the Fusion Breakpoint Selectively Depletes F3-T3, While Sparing WT FGFR3 and TACC3

Importantly, we wanted to ensure that treatment with iF3T3 did not result in depletion of WT FGFR3 or TACC3 to limit any possibility of normal tissue toxicity. To this end, we titrated increasing amounts of RNA and measured the ability of iF3T3 to degrade WT FGFR3 or TACC3. Specifically, we transfected SNB19.F3T3 and SNB19.WT FGFR3 cells with 25, 100, or 250 pmol iFGF3. As a positive

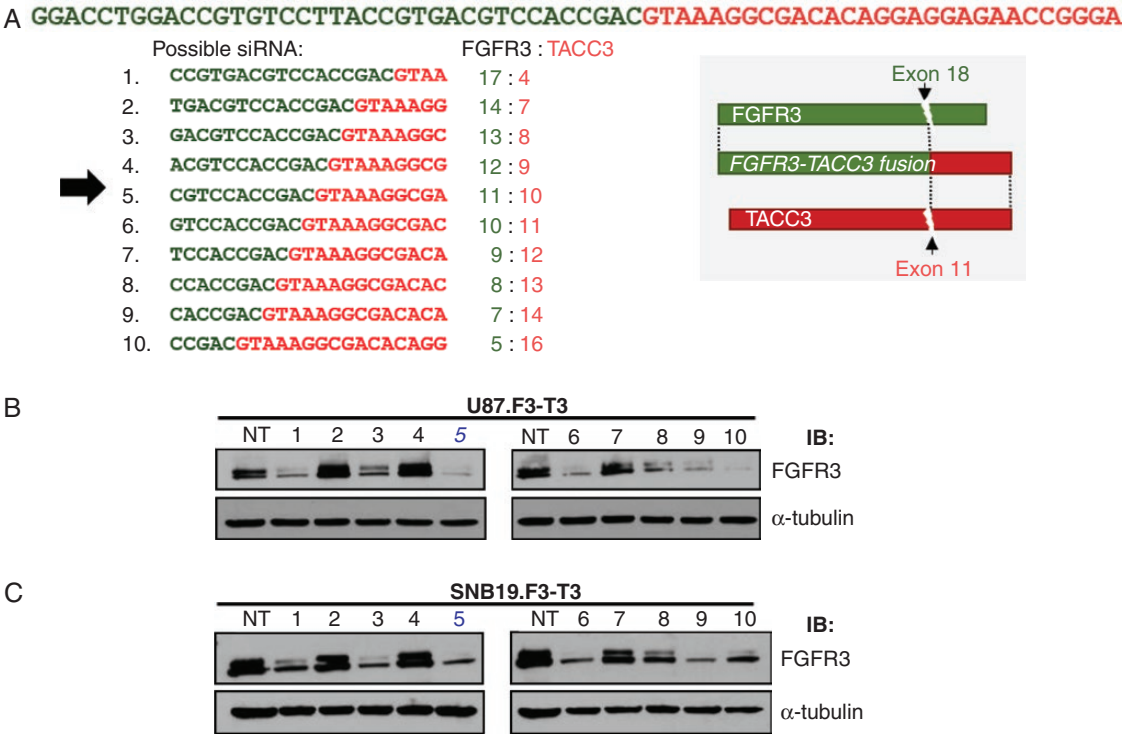

Figure 2. Designing siRNA to the F3-T3 fusion breakpoint. (A) Sequence of F3-T3 breakpoint and various custom siRNA constructs. Arrow points to construct #5, which was shown to be most effective in depleting F3-T3 protein in both U87.F3T3 (B) and SNB19.F3T3 (C) cell lines, as illustrated by immunoblotting.

control, siRNA to WT FGFR3 was transfected in a similar manner (Figure 3A and 3B). We engineered custom Taqman assays that selectively quantified either F3-T3 RNA or WT FGFR3 by designing primers that flanked the fusion junction or that flanked exons within FGFR3 that are lost upon formation of the fusion but are present in WT FGFR3, respectively (Supplementary Figure 5).

Cells were then harvested, RNA purified, and custom qPCR performed measuring relative levels of F3-T3 and WT FGFR3 RNA. Consistent with our previous results, transfection of SNB19.F3T3 cells with iF3T3 or si-FGFR3 resulted in depletion of F3-T3 RNA (Figure 3C). However, treatment of SNB19.WT FGFR3 cells resulted in depletion of WT FGFR3 only when si-FGFR3 was transfected, whereas transfection of iF3T3 had no effect even at doses of 250 pmol (Figure 3D). These results illustrate that iF3T3 selectively depletes F3-T3 RNA, and does not deplete WT FGFR3 RNA, overcoming concerns regarding normal tissue toxicity.

To further confirm that iF3T3 did not deplete WT FGFR3 or TACC3, we assessed FGFR3 and TACC3 protein levels. To this end, SNB19.F3T3 and SNB19.FGFR3 WT cells were transfected with 25, 100, or 250 pmol iFGF3 or siRNA to WT FGFR3. Protein lysates were analyzed via immunoblot 48 h later, and F3-T3 and WT FGFR3 were visualized by probing the blot with an antibody that recognized the N-terminal of FGFR3. Consistent with our previous results, transfection of SNB19.F3T3 with iF3T3 or si-FGFR3 resulted in depletion of F3-T3 protein. Notably, there were no differences in TACC3 protein expression observed, confirming iF3T3 does not deplete WT TACC3 (Figure 3E, Supplementary Figure 6). In contrast, analysis of SNB19.FGFR3 WT lysates shows that siRNA-FGFR3 depletes WT FGFR3 RNA, while iF3T3 does not. In agreement with SNB19.F3T3, treatment

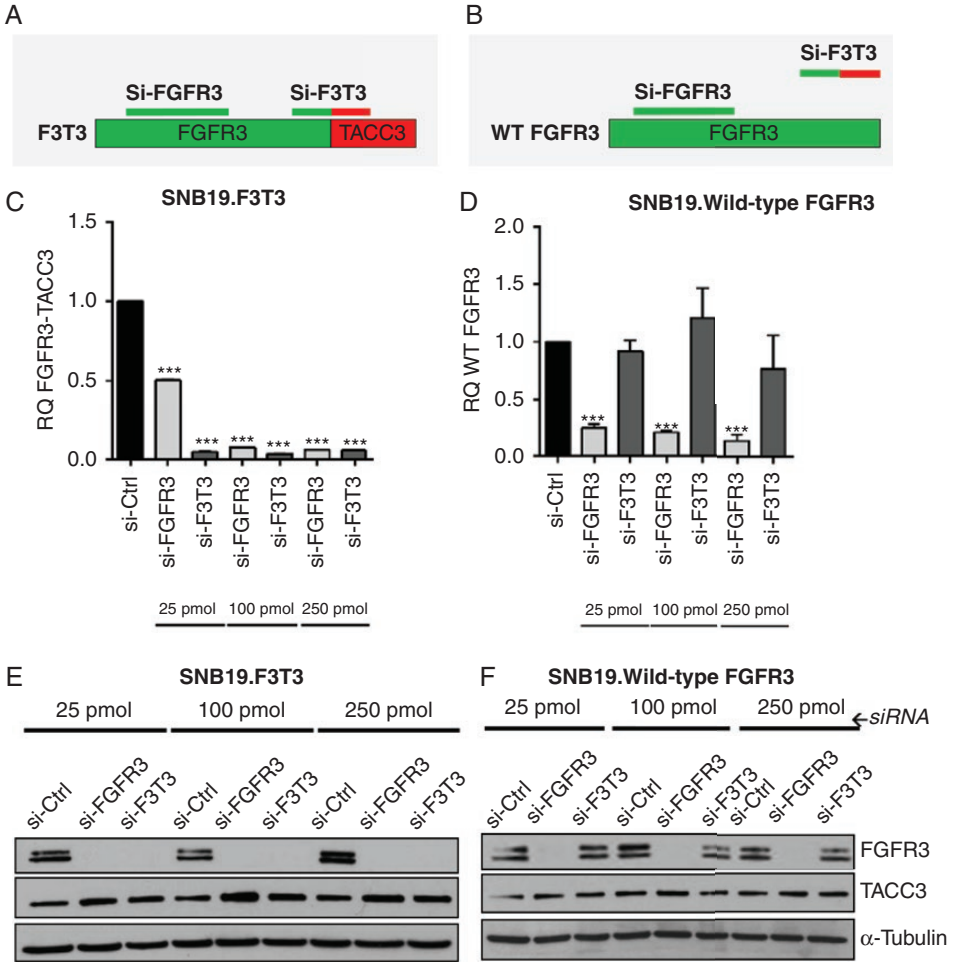

Figure 3. Transfection of iF3T3 results in depletion of F3-T3 but not WT FGFR3 RNA and WT FGFR3 and WT TACC3 protein. Schematic illustrating the location where si-FGFR3 or si-F3T3 target either F3-T3 (A) or WT FGFR3 (B) RNA constructs, respectively. (C) qPCR results illustrating F3-T3 RNA depletion in SNB19.F3T3 cells following treatment with increasing concentrations of both si-FGFR3 and si-F3T3. (D) qPCR results illustrating WT FGFR3 RNA depletion in SNB19.FGFR3 WT cells following treatment with increasing concentrations of si-FGFR3 but not si-F3T3. (E) Immunoblotting results illustrating F3-T3 depletion in SNB19.F3T3 cells following treatment with increasing concentrations of both si-FGFR3 and si-F3T3. Levels of WT TACC3 were also unchanged. (F) Immunoblotting results illustrating WT FGFR3 depletion in SNB19.FGFR3 WT cells following treatment with increasing concentrations of si-FGFR3 but not si-F3T3. ***$P < .0001$, unpaired *t*-test.

of SNB19.FGFR3 WT with either iF3T3 or siRNA-FGFR3 does not affect levels of TACC3 protein (Figure 3F).

Collectively, these results illustrate the potential of iF3T3 to deplete F3-T3 RNA and protein, while sparing WT FGFR3 and TACC3, suggesting the unique and promising potential of iF3T3 to inhibit F3-T3+ tumor cells while mitigating toxicity to normal tissues.

iF3T3-Mediated Depletion of F3T3 Results in Decreased Cell Viability

We hypothesized that treatment with RNAi targeting the fusion breakpoint is capable of inducing therapeutic cytotoxicity. To test this hypothesis, we utilized shRNA containing the same sequence as iF3T3 (sh-F3T3), as it would integrate and lead to sustained F3-T3 depletion over time. Specifically, U87.F3T3 or SNB19.F3T3 cell lines were treated with sh-F3T3 (3 MOI) and subject to cell viability assay. As expected, treatment with sh-F3T3 to the fusion breakpoint resulted in depletion of F3-T3 and decreased cell viability in both U87.F3T3 and SNB19.F3T3 cell lines compared with either no treatment or scrambled, non-targeting shRNA negative controls (Figure 4A–D).

To confirm that fusion-specific depletion technology was not unique to artificially created cell lines, we treated the bladder cancer cell line RT112 with sh-F3T3, as this cell line naturally contains the same common breakpoint that was engineered into U87.F3T3 and SNB19.F3T3 lines. Similar to what we observed with GBM lines, treatment of RT112 with sh-F3T3 resulted in decreased F3-T3 RNA, decreased F3-T3 protein, and decreased cell viability (Supplementary Figure 7).

Umbilical Cord Tissue-Derived Exosomes as Therapeutic Delivery Vehicle for iF3T3

Because naked RNA is degraded in blood and lacks directionality to organs of interest, we explored the ability to use exosomes derived from MSCs as delivery vehicles for iF3T3. To this end, MSCs were cultured and exosomes were isolated from the supernatant as described in Methods. Exosomes (1 µg total exosomes per well; ie, 5×10^8 exosomes per well) were loaded with iF3T3 by electroporation via multiple programs (indicated 1–4) and added to the media of U87.F3T3 cells. Lipofectamine mixed with iF3T3 was used as a positive control. Cells were then harvested, and RNA analyzed via RT-qPCR. Exosomes loaded with iF3T3 were able to successfully deliver functional iF3T3 that resulted in depletion of F3-T3 RNA, suggesting that this treatment strategy may prove effective for the delivery of iF3T3 (Figure 5). Future studies should examine the ability of exosomes loaded with iF3T3 to prolong survival in F3-T3+ tumor-bearing mice.

Discussion

Here, we show that RNAi that specifically targets the F3-T3 fusion breakpoint results in robust depletion of F3-T3 RNA/protein, while sparing WT FGFR3 and TACC3. This targeted RNAi causes death of F3-T3+ cells, but spares cells that do not harbor the fusion. Our results suggest that iF3T3 is a powerful therapeutic strategy because it has the potential to target tumor cells while limiting systemic toxicities. We also provide a mechanism to overcome historical barriers to drug delivery by testing the use of umbilical cord tissue-derived MSC exosomes to deliver iF3T3 to gliomas in vitro.

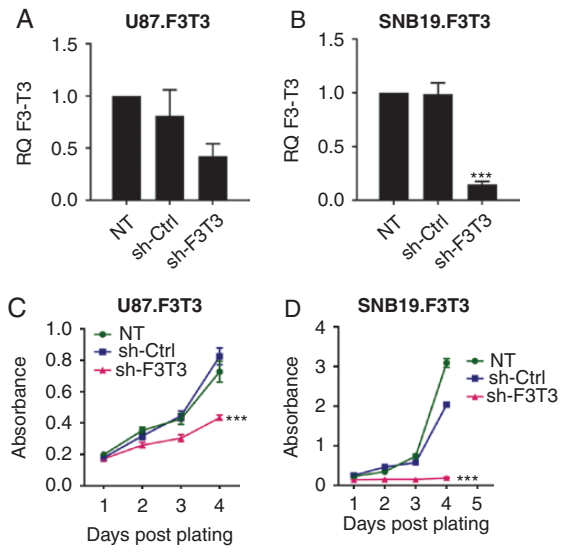

Figure 4. Targeted F3-T3 depletion results in decreased cell viability. F3-T3 RNA was decreased in U87.F3T3 (trending, $P = .09$) (A) and SNB19.F3T3 ($P < .0002$, unpaired *t*-test) (B) cells treated with sh-F3T3, which resulted in decreased cell viability in both lines, respectively (C,D) ***$P < .0001$, 2-way ANOVA.

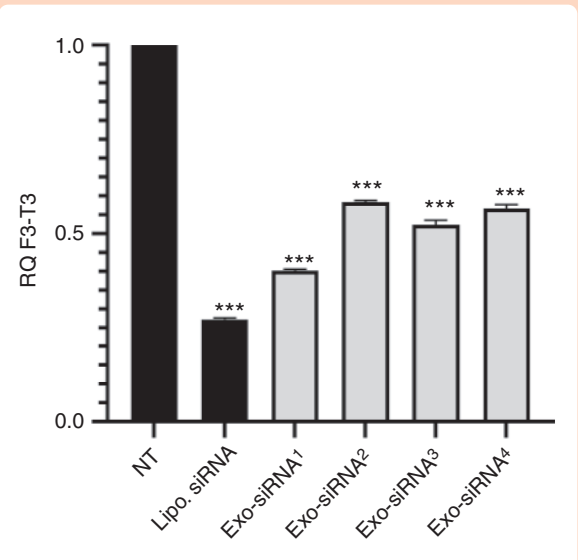

Figure 5. Umbilical cord tissue-derived MSC exosomes loaded with iF3T3 successfully deplete F3-T3 in vitro. qPCR assay illustrating that F3-T3 is depleted upon treatment with exosomes loaded with iF3T3 upon electroporation with electroporation programs 1–4. ***$P < .0001$, unpaired *t*-test.

Up to now, there has been no example of a successful targeted personalized therapeutic for GBM, and patients diagnosed with GBM typically experience a dismal prognosis of less than 14.6 months with the current standard of care. Personalized medicine strategies require identification of driver genes that may offer possibilities for actionable targets. One such driver event is the F3-T3 fusion, which not only occurs in a subset of GBMs, but also in several other cancer types.[9,10,12–16] Therefore, the identification of a therapy targeting this fusion gene may not only represents a targeted strategy for GBM, but may also offer a treatment strategy for all patients harboring this genetic alteration, regardless of the tumor of origin.

Traditional methods of personalized medicine involve the use of kinase inhibitors, which have been successful for the treatment of other fusion genes such as BCR-ABL, but unfortunately may lead to resistance and normal tissue toxicity. In fact, clinical trials assessing the efficacy and safety of targeting the F3-T3 fusion by small molecular inhibitors targeting the WT FGFR3 portion of the fusion protein have resulted in modest results primarily due to normal tissue toxicity. This is due to the fact that WT FGFR3 exists in several normal tissues throughout the body, and therefore strategies aimed at targeting the kinase portion of WT FGFR3 have led to normal tissue-related side effects. In contrast, here, we describe an RNAi-based strategy that specifically targets the fusion junction, and our data provide a strong rationale for the delivery of RNAi to fusion-positive patients. A similar approach has been developed for targeting the *TMPRSS2-ERG* fusion in prostate cancers with high success.[28] In our studies, even as low as 25 pmol siRNA leads to robust depletion of F3-T3 RNA and protein. We further showed that this strategy leads to decreased cell viability, both in GBM cell lines, where the fusion is forcibly overexpressed, and in the RT112 bladder cancer cell line, where the fusion is found naturally. Targeting F3-T3 fusion breakpoints whose sequence differs from the common breakpoint sequence, including the breakpoint sequences observed in MDA-GSC13 and MDA-GSC231 lines, would require the generation of RNAi that specifically target the breakpoint observed within those cases.

Importantly, we also showed that iF3T3 does not deplete levels of WT FGFR3 or TACC3, and therefore should not cause toxicity to normal tissues. Although WT FGFR3 levels are low in normal brain, it is found in various tissues throughout the body, and therefore, this therapeutic strategy has advantages over small-molecule inhibitors that target the kinase domain of WT FGFR3 and are associated with significant toxicity in nontumor tissues. Indeed, both infigratinib and dovitinib were stopped in 40%–70% of patients due to intolerable toxicity. The iF3T3 strategy should mitigate, if not eliminate, any normal tissue toxicity as the iF3T3 has no naturally occurring ligand to which to bind. Further testing in animal models is underway to explore this hypothesis.

Finally, we offer a strategy for siRNA delivery by using exosomes derived from cord-blood MSCs. Specifically, we show that siRNA loading into exosomes allows efficient depletion of F3-T3 RNA following treatment on F3-T3-positive GBM cells in vitro. The strategy of using MSC exosomes clinically has become very popular in recent decades, from treating type I diabetes (NCT02138331), and retinal injury (NCT03437759). Further, research from our laboratory showed that exosomes loaded with anti-glioma miR-124 are capable of homing to brain tumors and improving survival of tumor-bearing mice[26]. Therefore, this therapeutic strategy should be investigated further using animal models to determine the ability of MSC exosomes loaded with iF3T3 to promote survival of mice harboring these tumors.

In summary, we provide evidence of a strategy that specifically and robustly depletes F3-T3, while sparing WT FGFR3 and TACC3. Should in vivo models prove successful, this therapeutic strategy may be promising for the wide variety of cancers that harbor this oncogene. While we focus on the FGFR3-TACC3 fusion, our approach is applicable to all fusion proteins.

Supplementary Material

Supplementary material is available at *Neuro-Oncology Advances* online.

Keywords

FGFR3-TACC3 | fusion genes | glioblastoma | precision medicine | RNAi

Acknowledgments

Select data from this manuscript were presented at the American Chemical Society conference, August 2017.

Funding

This study was supported by grants from the National Cancer Institute (CA115729, R01CA214749, and 1P50 CA127001) and by the generous philanthropic contributions to The University of Texas MD Anderson Cancer Center Moon Shots Program™, The Broach Foundation for Brain Cancer Research, The Elias Family Fund, The Jason and Priscilla Hiley Fund, The Bauman Family Curefest fund, Chuanwei Lu Fund, The Sweet Family Fund, The Schneider Foundation, The Jim & Pam Harris Fund, The Gene Pennebaker Brain Cancer Fund, the Sorenson Foundation, and the Brian McCulloch Fund, the TLC Foundation and the Pappas Endowed Fund to F.F.L.

Conflict of interest statement. No conflicts of interest exist for any co-author on this manuscript.

Authorship Statement. B.C.P.K. conceived the study concept and overall hypothesis, performed experiments, oversaw the study design, and wrote the majority of the manuscript. D.L. performed select qPCR, electroporation experiments, assisted with animal experiments, and contributed to writing the manuscript. M.K. performed select immunoblotting experiments. L.P. performed select qPCR experiments and helped with experimental design. J.G. performed animal study experiments. A.H. assisted with virus production and experimental design. J.Y. assisted with cell culture maintenance. M.M. assisted with electroporation experiments and assisted with experimental design of electroporation design. S.S. performed RNAseq analysis on Glioma Stem-like Cell (GSC) lines. D.C. assisted with the identification of F3-T3-positive GSCs. C.E. provided clinical expertise and assisted in writing portions of the manuscript. E.S. is the Director of the Cell Therapy Laboratory and Director of the Cord Blood Bank at The University of Texas MD Anderson Cancer Center, and assisted with overall rationale and design of electroporation experiments. F.F.L. is the laboratory Principal Investigator, edited and approved the final manuscript and provided overall study oversight.

References

1. Parker BC, Zhang W. Fusion genes in solid tumors: an emerging target for cancer diagnosis and treatment. *Chin J Cancer.* 2013;32(11):594–603.
2. Annala MJ, Parker BC, Zhang W, Nykter M. Fusion genes and their discovery using high throughput sequencing. *Cancer Lett.* 2013;340(2):192–200.
3. Croce CM. Chromosome translocations and human cancer. *Cancer Res.* 1986;46(12 Pt 1):6019–6023.
4. Shtivelman E, Lifshitz B, Gale RP, Canaani E. Fused transcript of abl and bcr genes in chronic myelogenous leukaemia. *Nature.* 1985;315(6020):550–554.
5. Soda M, Choi YL, Enomoto M, et al. Identification of the transforming EML4-ALK fusion gene in non-small-cell lung cancer. *Nature.* 2007;448(7153):561–566.
6. Camidge DR, Bang YJ, Kwak EL, et al. Activity and safety of crizotinib in patients with ALK-positive non-small-cell lung cancer: updated results from a phase 1 study. *Lancet Oncol.* 2012;13(10):1011–1019.
7. Shaw AT, Engelman JA. Ceritinib in ALK-rearranged non-small-cell lung cancer. *N Engl J Med.* 2014;370(26):2537–2539.
8. Shaw AT, Yeap BY, Solomon BJ, et al. Effect of crizotinib on overall survival in patients with advanced non-small-cell lung cancer harbouring ALK gene rearrangement: a retrospective analysis. *Lancet Oncol.* 2011;12(11):1004–1012.
9. Parker BC, Annala MJ, Cogdell DE, et al. The tumorigenic FGFR3-TACC3 gene fusion escapes miR-99a regulation in glioblastoma. *J Clin Invest.* 2013;123(2):855–865.
10. Singh D, Chan JM, Zoppoli P, et al. Transforming fusions of FGFR and TACC genes in human glioblastoma. *Science.* 2012;337(6099):1231–1235.
11. Parker BC, Engels M, Annala M, Zhang W. Emergence of FGFR family gene fusions as therapeutic targets in a wide spectrum of solid tumours. *J Pathol.* 2014;232(1):4–15.
12. Williams SV, Hurst CD, Knowles MA. Oncogenic FGFR3 gene fusions in bladder cancer. *Hum Mol Genet.* 2013;22(4):795–803.
13. Majewski IJ, Mittempergher L, Davidson NM, et al. Identification of recurrent FGFR3 fusion genes in lung cancer through kinome-centred RNA sequencing. *J Pathol.* 2013;230(3):270–276.
14. Wu YM, Su F, Kalyana-Sundaram S, et al. Identification of targetable FGFR gene fusions in diverse cancers. *Cancer Discov.* 2013;3(6):636–647.
15. Yuan L, Liu ZH, Lin ZR, Xu LH, Zhong Q, Zeng MS. Recurrent FGFR3-TACC3 fusion gene in nasopharyngeal carcinoma. *Cancer Biol Ther.* 2014;15(12):1613–1621.
16. Yoshihara K, Wang Q, Torres-Garcia W, et al. The landscape and therapeutic relevance of cancer-associated transcript fusions. *Oncogene.* 2015;34(37):4845–4854.
17. Stupp R, Mason WP, van den Bent MJ, et al. Radiotherapy plus concomitant and adjuvant temozolomide for glioblastoma. *N Engl J Med.* 2005;352(10):987–996.
18. Lassman A, Sepulveda-Sanchez J, Cloughesy T, et al. Infigratinib (Bgj398) in patients with recurrent gliomas with fibroblast growth factor receptor (Fgfr) alterations: a multicenter phase II study. *Neuro Oncol.* 2019;21(20-20):iii21–iii22.
19. Sharma M, Schilero C, Peereboom DM, et al. Phase II study of Dovitinib in recurrent glioblastoma. *J Neurooncol.* 2019;144(2):359–368.
20. van Linde ME, Brahm CG, de Witt Hamer PC, et al. Treatment outcome of patients with recurrent glioblastoma multiforme: a retrospective multicenter analysis. *J Neurooncol.* 2017;135(1):183–192.
21. Nakamizo A, Marini F, Amano T, et al. Human bone marrow-derived mesenchymal stem cells in the treatment of gliomas. *Cancer Res.* 2005;65(8):3307–3318.
22. Hata N, Shinojima N, Gumin J, et al. Platelet-derived growth factor BB mediates the tropism of human mesenchymal stem cells for malignant gliomas. *Neurosurgery.* 2010;66(1):144–56; discussion 156.
23. Doucette T, Rao G, Yang Y, et al. Mesenchymal stem cells display tumor-specific tropism in an RCAS/Ntv-a glioma model. *Neoplasia.* 2011;13(8):716–725.
24. Shinojima N, Hossain A, Takezaki T, et al. TGF-β mediates homing of bone marrow-derived human mesenchymal stem cells to glioma stem cells. *Cancer Res.* 2013;73(7):2333–2344.
25. Yong RL, Shinojima N, Fueyo J, et al. Human bone marrow-derived mesenchymal stem cells for intravascular delivery of oncolytic adenovirus Delta24-RGD to human gliomas. *Cancer Res.* 2009;69(23):8932–8940.
26. Lang FM, Hossain A, Gumin J, et al. Mesenchymal stem cells as natural biofactories for exosomes carrying miR-124a in the treatment of gliomas. *Neuro Oncol.* 2018;20(3):380–390.
27. Milowsky MI, Dittrich C, Durán I, et al. Phase 2 trial of dovitinib in patients with progressive FGFR3-mutated or FGFR3 wild-type advanced urothelial carcinoma. *Eur J Cancer.* 2014;50(18):3145–3152.
28. Urbinati G, Ali HM, Rousseau Q, et al. Antineoplastic effects of siRNA against TMPRSS2-ERG junction oncogene in prostate cancer. *PLoS One.* 2015;10(5):e0125277.